Choosing the Right Strategy: Cryogrinding vs Ball Milling – Comparing Apples to Apples

Julia L. Shamshina[a,*], Robin S. Stein[b], and Noureddine Abidi[a]

Fiber and Biopolymer Research Institute, Department of Plant and Soil Science, Texas Tech University, Lubbock, Texas, USA 79409

McGill University, Department of Chemistry, Montreal, QC H3A0B8, Canada

Supplementary Information (SI)

Table S1. Chemical composition ranges of grade 440 stainless steels, %

Grade	C	Mn	Si	P	S	Cr	Mo	Ni
440 C	0.95 – 1.20	0 – 1	0 – 1	0 – 0.04	0 – 0.03	16 – 18	0 – 0.75	0

Table S2. Chitin dissolution in [C_2mim][OAc] ionic liquid.

# Cycles	IL, g	Chitin, g	Conc., wt%[a]
0	9.904	0.094	1.01
3	9.908	0.093	1.01
6	9.907	0.095	1.03
12	9.902	0.096	1.01
24	9.914	0.096	1.01

The concentration (wt%) was calculated as a ratio between amount of dry chitin to the total amount of solution (i.e., sum of chitin mass and the IL mass), according to formula: *(wt%)* $= \frac{m_{chitin}}{m_{chitin} + m_{IL}} \times 100\%$.

Table S3. List of chitin FTIR peaks

	Cardenas *et al.*[i]	Kaya *et al.*[ii]	Akpan *et al.*[iii]
O—H stretch	3448	3433	3449
N—H (as.) stretch	3268	3260	3263
N—H (sym.) stretch	3102	3104	3103
C—H (CH_3, asym.) stretch	2965		
C—H (CH_3, sym.) stretch	2880	2875	2853
C—H (CH_2, asym.) stretch	2929	2940	2926
C=O stretch (amide I), C(O)…HN	1656	1652	1653
C=O stretch (amide I), RCH_2OH…C(O)…HN	1627	1620	1620
C—N stretch (amide II) + N—H bend	1556	1552	1563
CH_3/ CH_2 bending	1424, 1376	1420, 1375	1378
N—H (amide III) bending	1314	1307	1309
C—O—C (asymmetric bridging, ring) stretch	1155	1154	
C—O (asymmetric in plane ring) stretch	1111	1112	
C3—OH stretch	1069	1067	1077
C6—OH stretch	1032	1027	1027
CH_3 wagging	948	951	

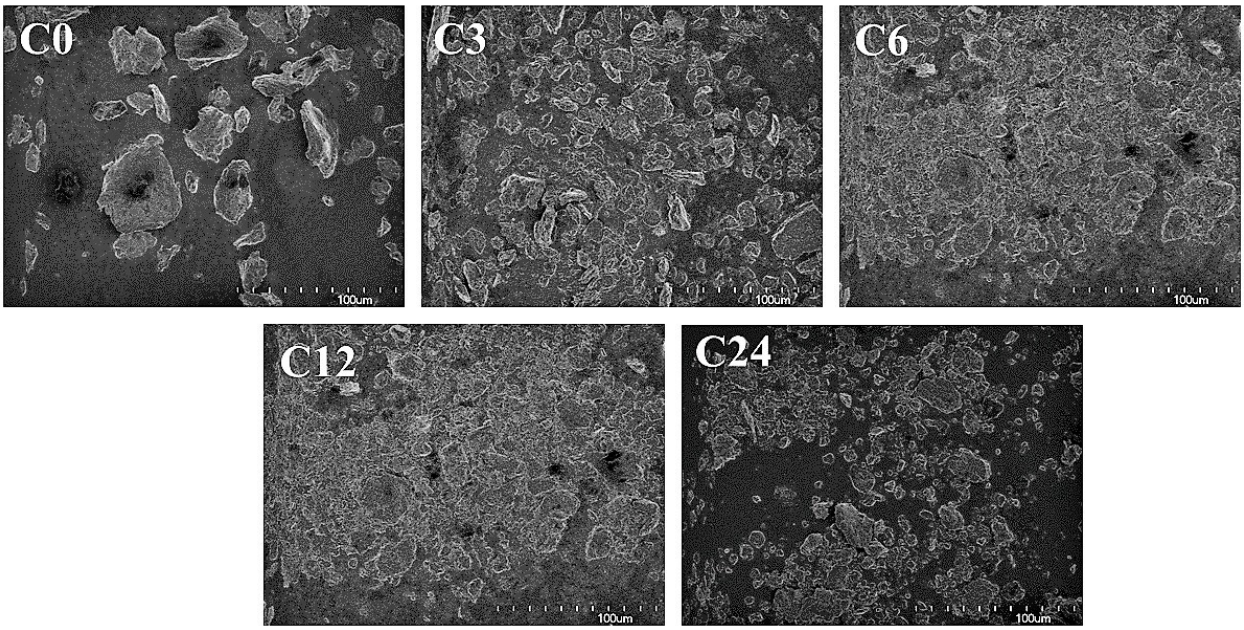

Figure S1. Hitachi S-4700 images of cryoground chitin. Magnification: 500, Accelerating Voltage: 2000, Emission Current: 9000, Working Distance: 12000, Lens Mode: Normal.

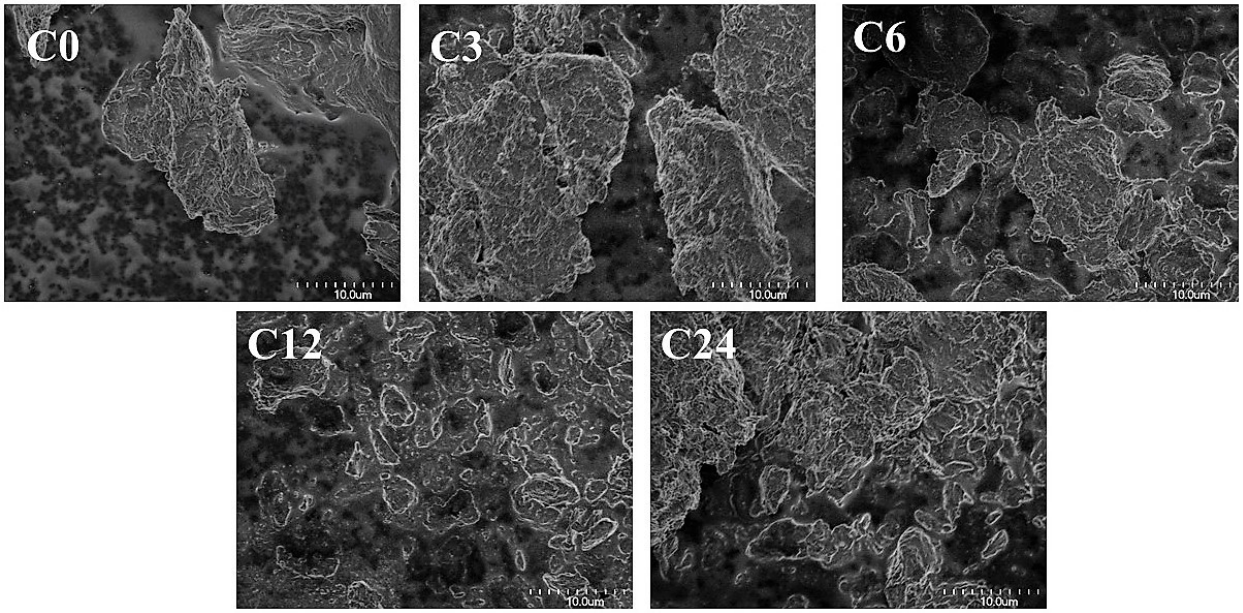

Figure S2. Hitachi S-4700 images of cryoground chitin. Magnification: 3000, Accelerating Voltage: 2000, Emission Current: 8500, Working Distance: 12000, Lens Mode: Normal.

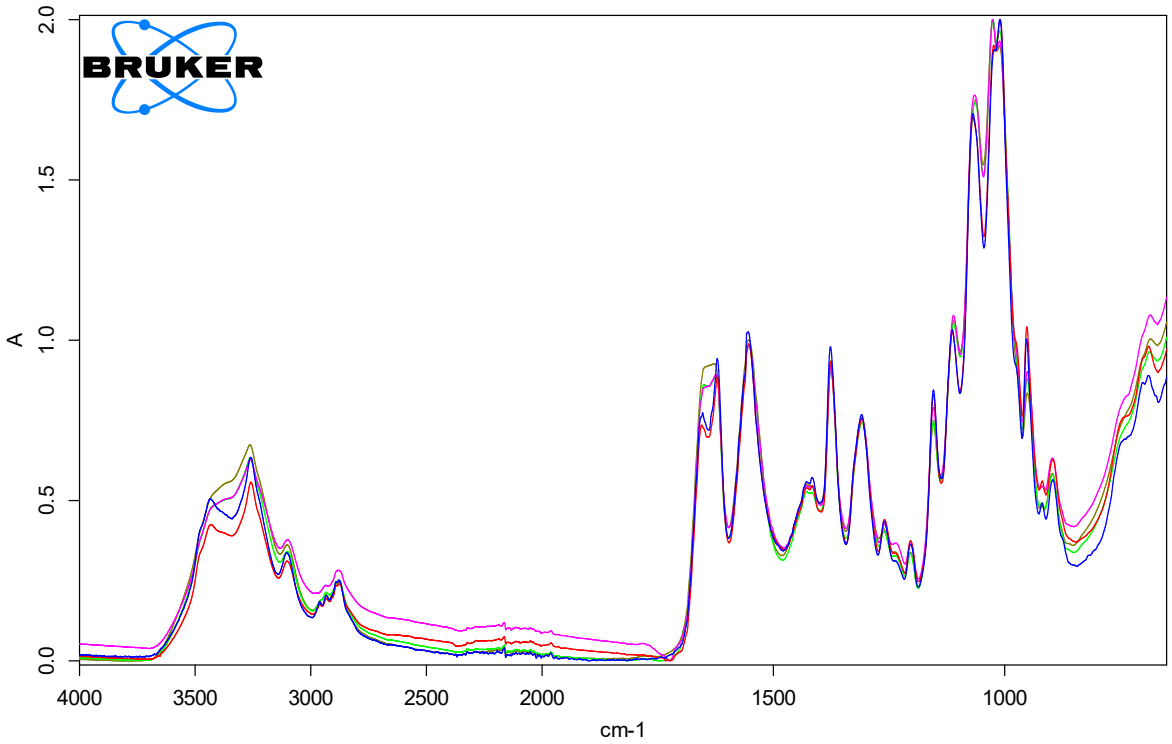

Figure S3. ATR FT-IR spectra for cryoground chitin: C0 (blue), C3 (red), C6 (pink), C12 (green), and C24 (mustard), full spectra in the range 4000 – 600 cm^{-1}.

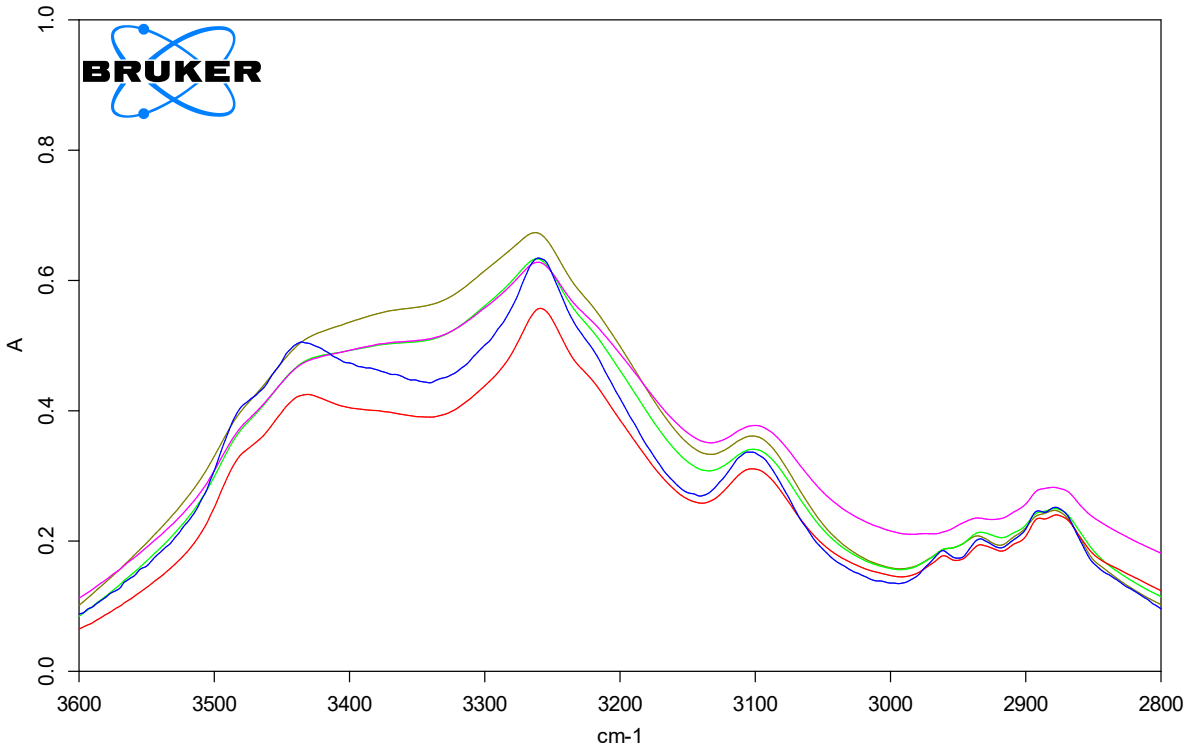

Figure S4. ATR FT-IR spectra for cryoground chitin: C0 (blue), C3 (red), C6 (pink), C12 (green), and C24 (mustard), O—H stretching region 3600 – 3800 cm^{-1}.

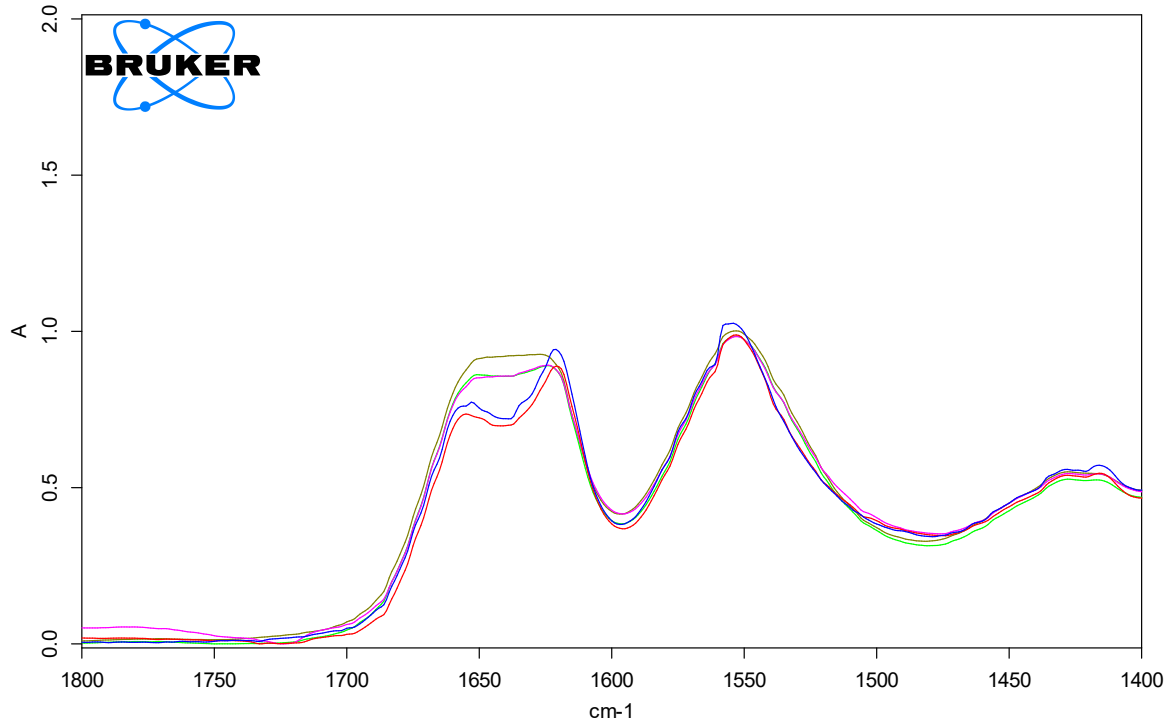

Figure S5. ATR FT-IR spectra for cryoground chitin: C0 (blue), C3 (red), C6 (pink), C12 (green), and C24 (mustard), vibration modes of amide I in the region 1660 –1620 cm^{-1}. Shown is expanded region 1800 – 1400 cm^{-1}.

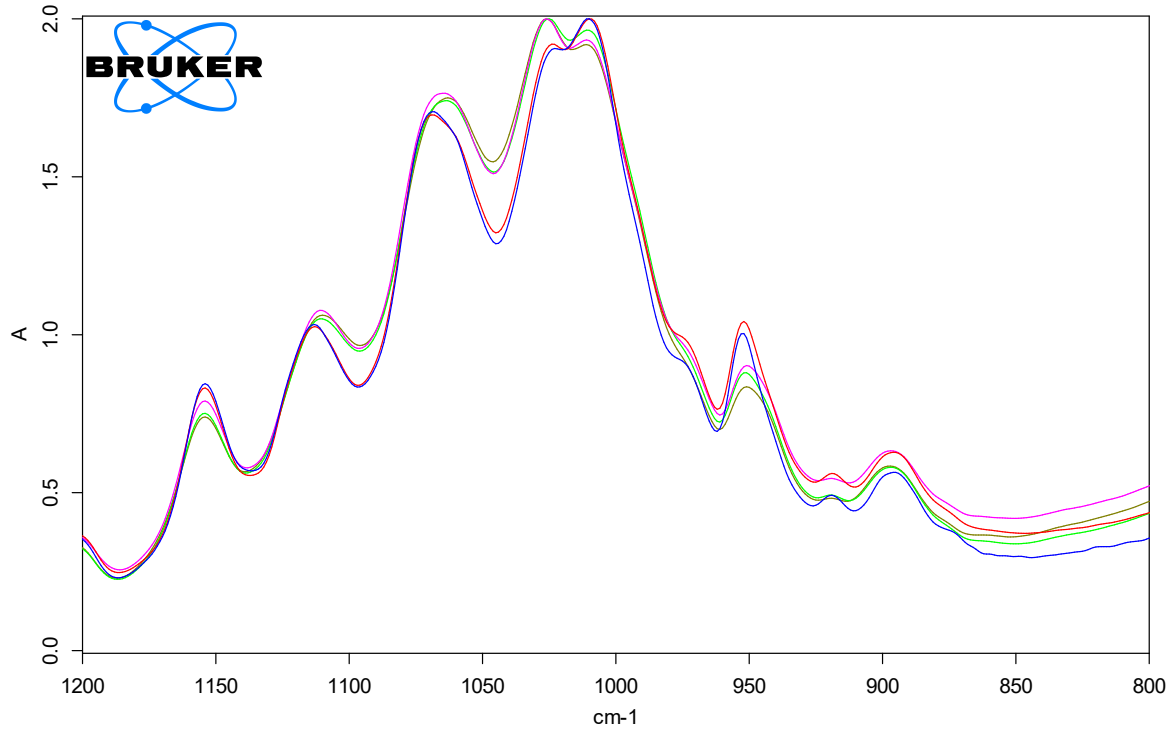

Figure S6. ATR FT-IR spectra for cryoground chitin: C0 (blue), C3 (red), C6 (pink), C12 (green), and C24 (mustard), in the region 1200 –800 cm^{-1}.

Table S4. CrI from the height ratio between the maximum intensity (arbitrary units) of the diffraction (110) at 2Θ 19.2° and intensity of the amorphous diffraction at 2Θ 12.6°

	I_{110} Intensity at 2θ = 19.2°	**I_{am} (Method 1): Intensity at 2θ = 12.6°**	**CrI**
C0	1.0000	0.0870	91.3
C3	1.0000	0.0870	91.3
C6	1.0000	0.1260	87.4
C12	1.0000	0.1180	88.2
C24	1.0000	0.2260	77.4

Table S5. CrI from the height ratio between the maximum intensity (arbitrary units) of the diffraction (110) at 2Θ 19.2° and a baseline height at 2Θ 16.0°

	I_{110} Intensity at 2θ = 19.2°	**I_{am} (Method 2): Intensity at 2θ = 16°**	**CrI**
C0	1.0000	0.0098	99.0
C3	1.0000	0.0180	98.2
C6	1.0000	0.0200	98.0
C12	1.0000	0.0360	96.4
C24	1.0000	0.1750	82.5

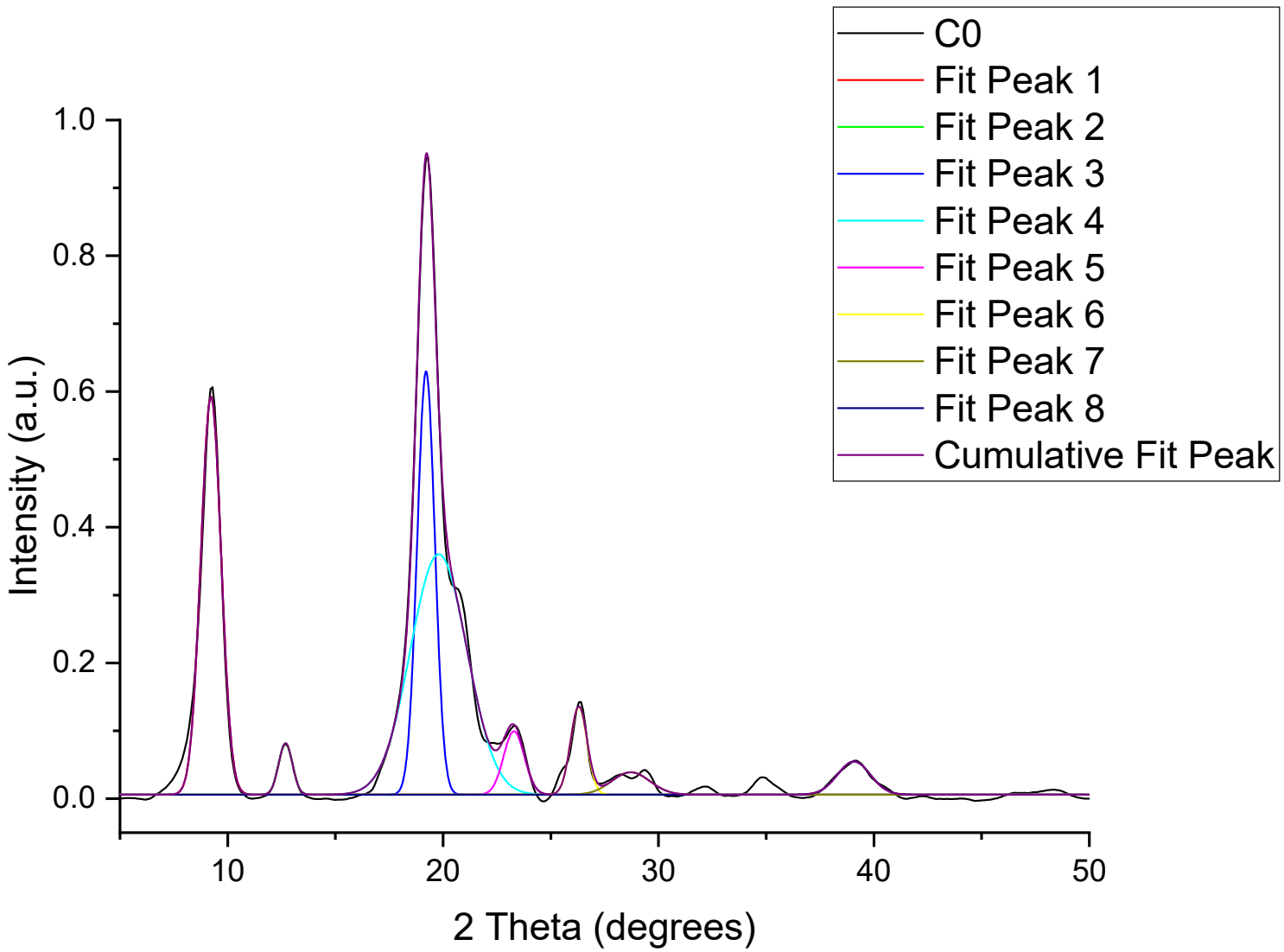

Figure S7. pXRD diffractogram for cryoground chitin: C0.

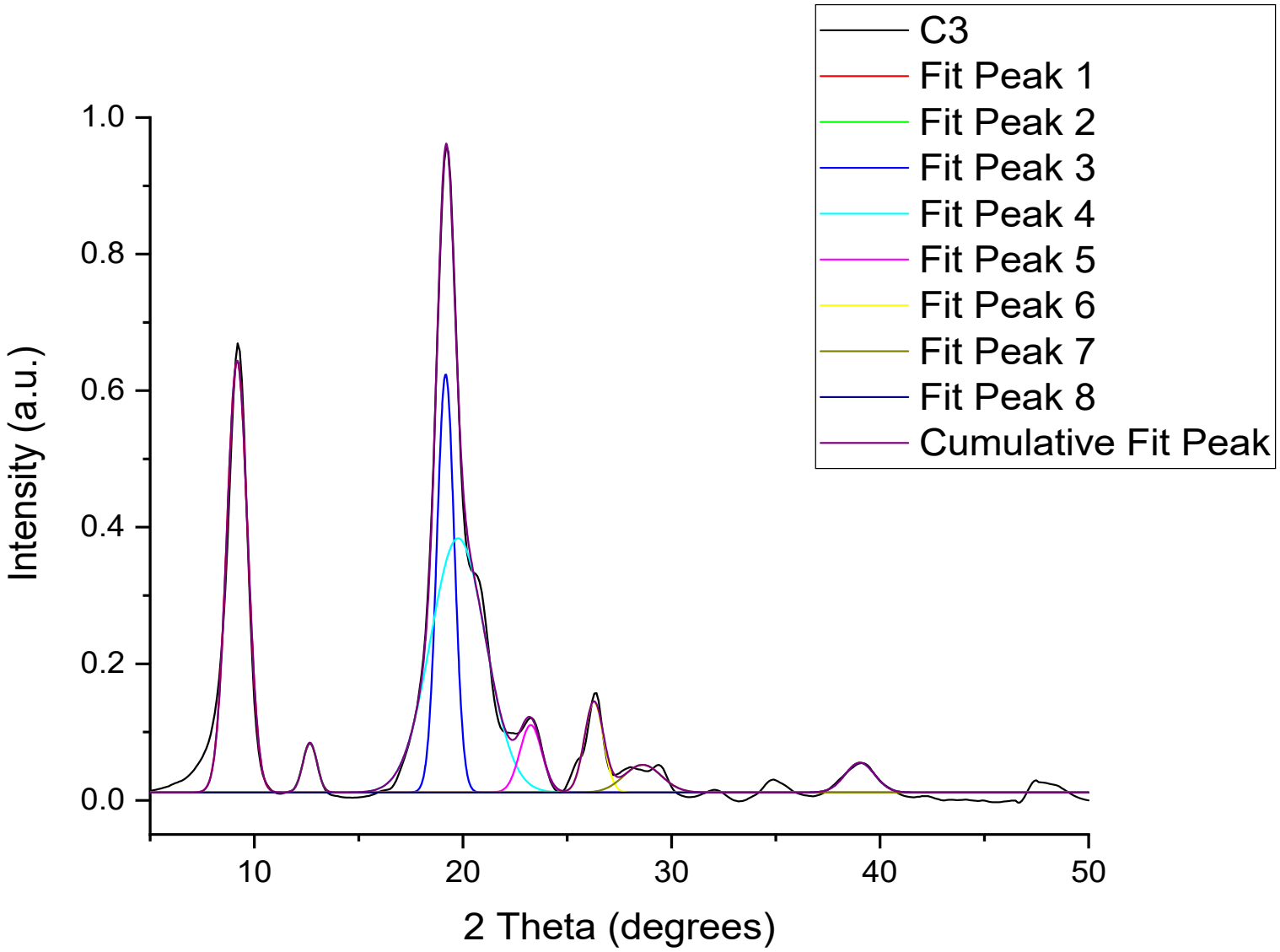

Figure S8. pXRD diffractogram for cryoground chitin: C3.

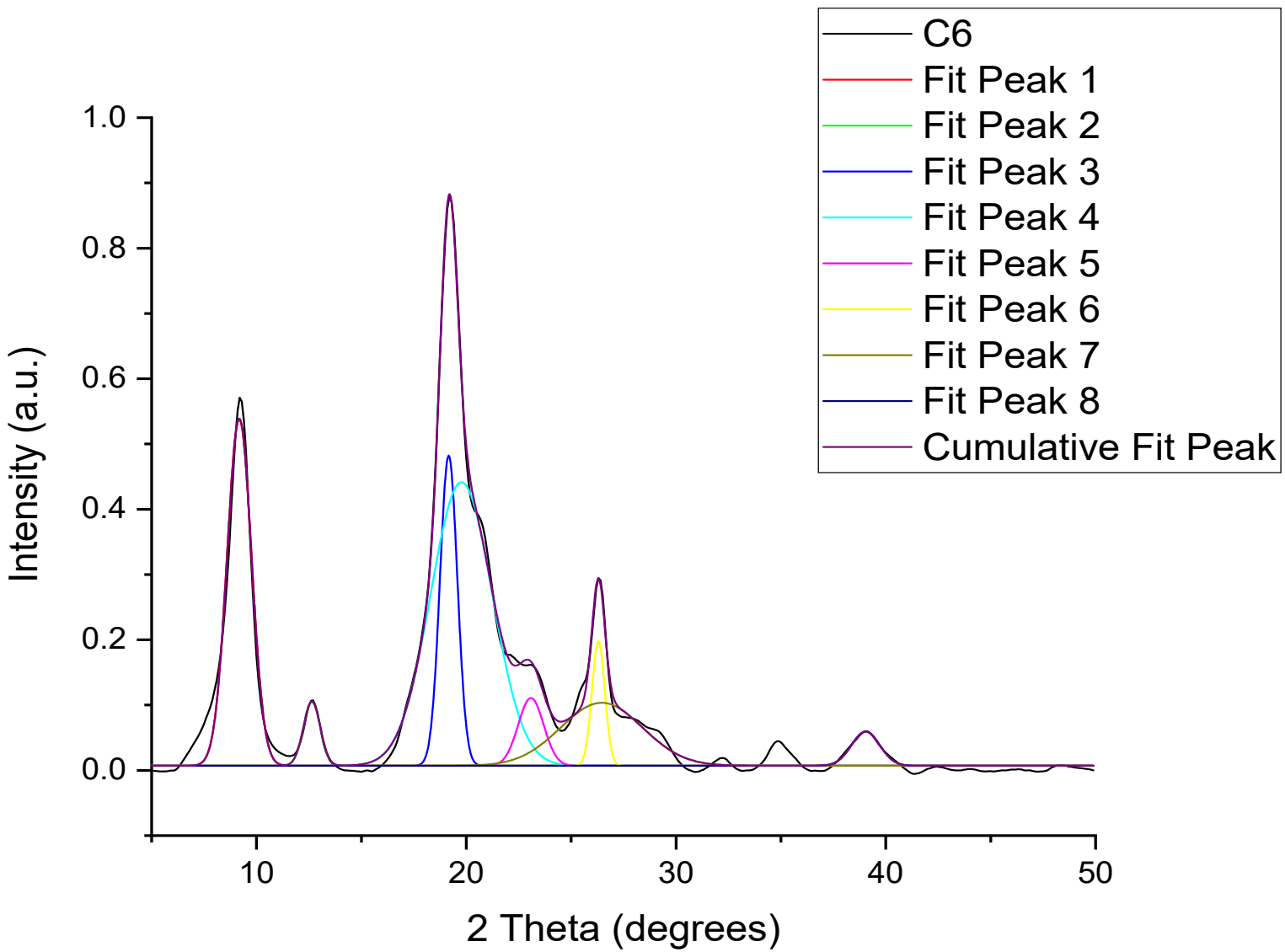

Figure S9. pXRD diffractogram for cryoground chitin: C6

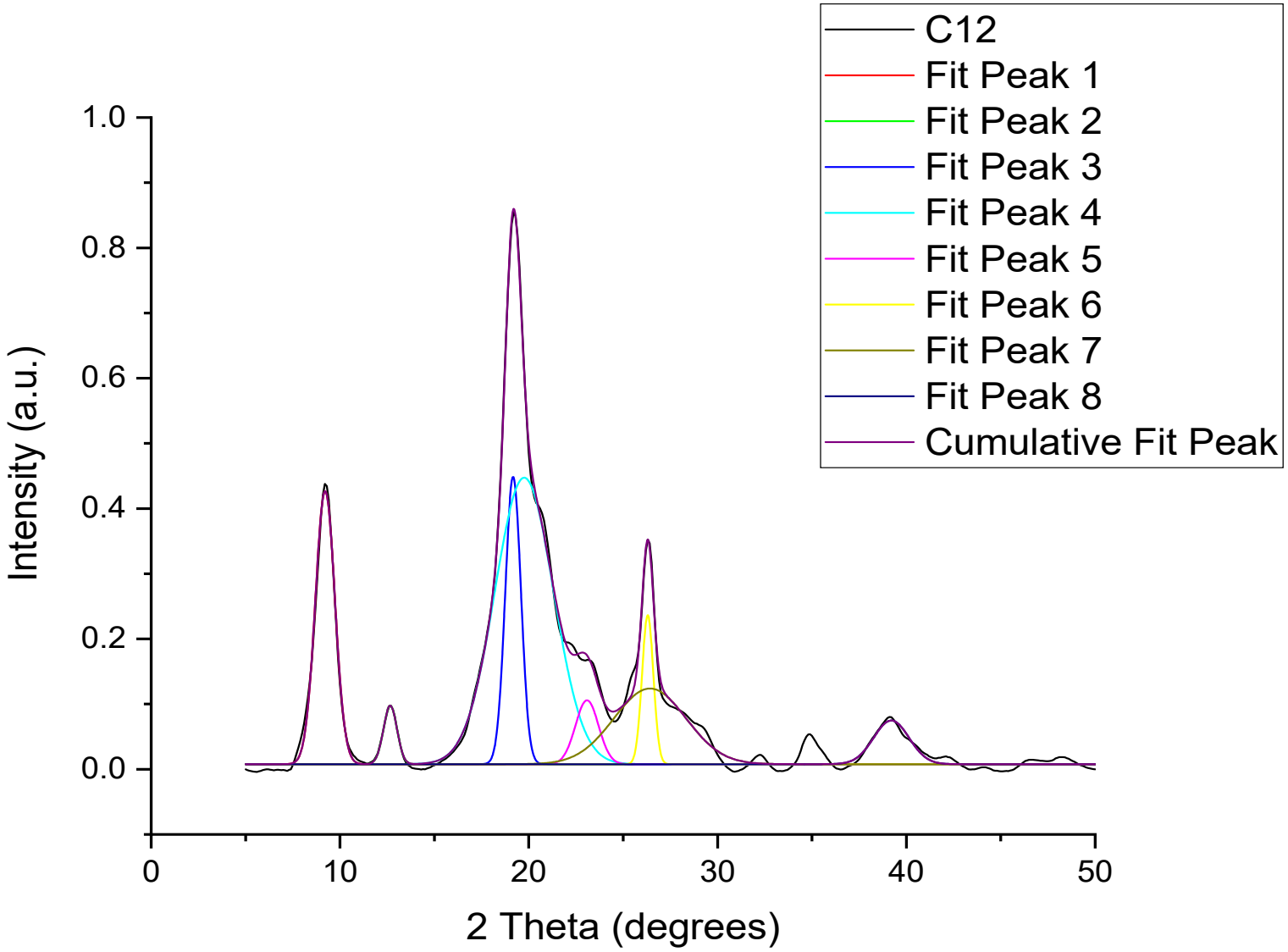

Figure S10. pXRD diffractogram for cryoground chitin: C12

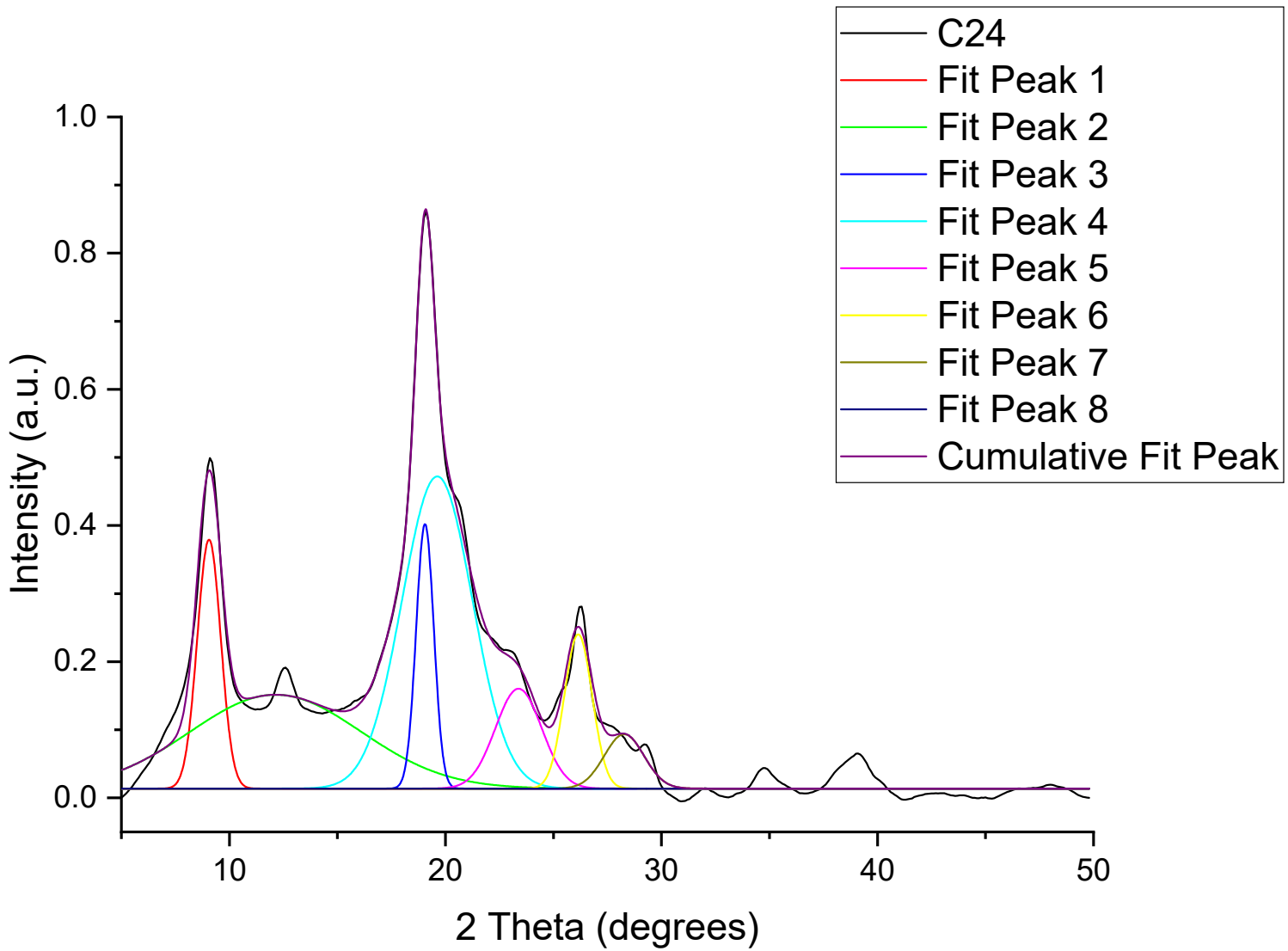

Figure S11. pXRD diffractogram for cryoground chitin: C24

Table S6. pXRD diffractogram for cryoground chitin: peak fitting parameters and CrI values

	Sample	C0		C3		C6		C12		C24	
Peak Number and Position	**Parameter**	**Value**	**Standard Error**	**Value**	**Standard Error**	**Value**	**Standard Error**	**Value**	**Standard Error**	**Value**	**Standard Error**
Peak 1, 9.2 °	**y0**	0.0060	0.0007	0.0115	0.0009	0.0070	0.0010	0.0078	0.0008	0.0137	0.0012
	xc	9.2238	0.0043	9.1736	0.0053	9.1773	0.0069	9.2147	0.0062	9.0567	0.0115
	w	0.9383	0.0088	0.9908	0.0107	1.1659	0.0142	1.0333	0.0128	1.0873	0.0261
	Area	0.6892	0.0058	0.7855	0.0076	0.7768	0.0086	0.5425	0.0061	0.4984	0.0132
	sigma	0.4691	0.0044	0.4954	0.0054	0.5829	0.0071	0.5166	0.0064	0.5437	0.0131
	FWHM	1.1047	0.0103	1.1666	0.0126	1.3727	0.0167	1.2166	0.0150	1.2802	0.0308
	Height	0.5861	0.0047	0.6326	0.0058	0.5316	0.0055	0.4189	0.0044	0.3657	0.0070
Peak 2, 12.6 °	**y0**	0.0060	0.0007	0.0115	0.0009	0.0070	0.0010	0.0078	0.0008	0.0137	0.0012
	xc	12.6857	0.0273	12.6588	0.0372	12.6376	0.0310	12.6603	0.0240	12.1402	0.1775
	w	0.6305	0.0553	0.6622	0.0753	0.8012	0.0631	0.7088	0.0487	7.9139	0.3508
	Area	0.0599	0.0047	0.0606	0.0061	0.0988	0.0070	0.0800	0.0049	1.3668	0.0546
	sigma	0.3153	0.0276	0.3311	0.0376	0.4006	0.0316	0.3544	0.0244	3.9570	0.1754
	FWHM	0.7424	0.0651	0.7797	0.0886	0.9434	0.0743	0.8345	0.0574	9.3179	0.4130
	Height	0.0759	0.0057	0.0730	0.0071	0.0984	0.0066	0.0901	0.0053	0.1378	0.0032
Peak 3, 19.2 °	**y0**	0.0060	0.0007	0.0115	0.0009	0.0070	0.0010	0.0078	0.0008	0.0137	0.0012
	xc	19.2084	0.0045	19.1682	0.0059	19.1604	0.0074	19.1701	0.0059	19.0532	0.0102
	w	0.8159	0.0120	0.8283	0.0160	0.8267	0.0214	0.8249	0.0172	0.8162	0.0315
	Area	0.6380	0.0149	0.6362	0.0197	0.4924	0.0205	0.4561	0.0151	0.3974	0.0260
	sigma	0.4080	0.0060	0.4141	0.0080	0.4134	0.0107	0.4124	0.0086	0.4081	0.0158
	FWHM	0.9607	0.0141	0.9752	0.0188	0.9734	0.0252	0.9712	0.0202	0.9610	0.0371
	Height	0.6239	0.0083	0.6128	0.0108	0.4752	0.0112	0.4411	0.0082	0.3885	0.0143
Peak 4, 19.8 °	**y0**	0.0060	0.0007	0.0115	0.0009	0.0070	0.0010	0.0078	0.0008	0.0137	0.0012
	xc	19.7970	0.0199	19.7673	0.0253	19.7702	0.0276	19.7579	0.0213	19.6217	0.0536
	w	2.6149	0.0360	2.6327	0.0460	2.9364	0.0566	3.0979	0.0463	3.2488	0.1336
	Area	1.1608	0.0169	1.2283	0.0219	1.5987	0.0211	1.7067	0.0157	1.8665	0.0591
	sigma	1.3074	0.0180	1.3163	0.0230	1.4682	0.0283	1.5490	0.0232	1.6244	0.0668
	FWHM	3.0788	0.0424	3.0997	0.0541	3.4574	0.0666	3.6475	0.0545	3.8251	0.1573
	Height	0.3542	0.0074	0.3723	0.0098	0.4344	0.0100	0.4396	0.0073	0.4584	0.0114

Peak 5, 23.2 °	**y0**	0.0060	0.0007	0.0115	0.0009	0.0070	0.0010	0.0078	0.0008	0.0137	0.0012
	xc	23.2891	0.0291	23.2499	0.0378	23.0811	0.0478	23.0838	0.0386	23.3848	0.0945
	w	0.9570	0.0595	1.0492	0.0773	1.2102	0.1102	1.2213	0.0899	2.1404	0.2181
	Area	0.1120	0.0066	0.1299	0.0092	0.1575	0.0199	0.1501	0.0159	0.3934	0.0532
	sigma	0.4785	0.0298	0.5246	0.0386	0.6051	0.0551	0.6107	0.0450	1.0702	0.1091
	FWHM	1.1268	0.0701	1.2353	0.0910	1.4249	0.1298	1.4380	0.1058	2.5202	0.2568
	Height	0.0934	0.0047	0.0988	0.0057	0.1038	0.0074	0.0981	0.0058	0.1466	0.0082
Peak 6, 26.3 °	**y0**	0.0060	0.0007	0.0115	0.0009	0.0070	0.0010	0.0078	0.0008	0.0137	0.0012
	xc	26.2997	0.0187	26.2783	0.0274	26.2965	0.0146	26.3000	0.0090	26.1480	0.0373
	w	0.7702	0.0380	0.9157	0.0552	0.6145	0.0344	0.5997	0.0214	1.2856	0.0814
	Area	0.1249	0.0056	0.1518	0.0088	0.1471	0.0097	0.1719	0.0073	0.3650	0.0300
	sigma	0.3851	0.0190	0.4579	0.0276	0.3073	0.0172	0.2998	0.0107	0.6428	0.0407
	FWHM	0.9068	0.0447	1.0782	0.0650	0.7236	0.0405	0.7060	0.0252	1.5137	0.0959
	Height	0.1294	0.0052	0.1323	0.0061	0.1909	0.0085	0.2288	0.0065	0.2265	0.0083
Peak 7, 28.7 °	**y0**	0.0060	0.0007	0.0115	0.0009	0.0070	0.0010	0.0078	0.0008	0.0137	0.0012
	xc	28.7122	0.1097	28.6117	0.1241	26.4519	0.1077	26.4200	0.0667	28.2721	0.1413
	w	1.7663	0.2402	1.7940	0.2786	3.9046	0.2652	3.8164	0.1661	1.8342	0.2622
	Area	0.0731	0.0086	0.0910	0.0120	0.4721	0.0256	0.5553	0.0190	0.1835	0.0259
	sigma	0.8832	0.1201	0.8970	0.1393	1.9523	0.1326	1.9082	0.0831	0.9171	0.1311
	FWHM	2.0797	0.2828	2.1122	0.3280	4.5974	0.3123	4.4934	0.1956	2.1596	0.3087
	Height	0.0330	0.0035	0.0405	0.0045	0.0965	0.0052	0.1161	0.0040	0.0798	0.0053
Peak 8, 39.03 °	**y0**	0.0060	0.0007	0.0115	0.0009	0.0070	0.0010	0.0078	0.0008	0.0137	0.0012
	xc	39.0734	0.0659	39.0323	0.0911	39.0376	0.0754	39.2034	0.0524	39.0869	0.0000
	w	1.5214	0.1356	1.4153	0.1871	1.3421	0.1551	1.8713	0.1092	0.0010	0.0000
	Area	0.0931	0.0076	0.0773	0.0093	0.0881	0.0093	0.1572	0.0085	0.0088	0.0000
	sigma	0.7607	0.0678	0.7077	0.0936	0.6711	0.0775	0.9356	0.0546	0.0005	0.0000
	FWHM	1.7913	0.1597	1.6664	0.2203	1.5802	0.1826	2.2033	0.1285	0.0012	0.0000
	Height	0.0488	0.0037	0.0436	0.0049	0.0524	0.0052	0.0670	0.0033	6.9413	0.0000
Area under peaks		**4.1117**		**4.3890**		**5.4302**		**5.5266**		**6.9462**	
Cryst. Peaks Area		**2.7848**		**2.9924**		**3.2713**		**3.1074**		**3.5206**	
% CrI		**67.7280**		**68.1794**		**60.2417**		**56.2264**		**50.6835**	

Table S7. Crystallite size (110)

Cycles	2Θ, °	Θ, °	Θ, radians	cos Θ	FWHM, °	FWHM, radians	Size, nm
0	19.20	9.60	0.1676	0.9860	0.9607	0.0168	84.77
3	19.20	9.60	0.1676	0.9860	0.9752	0.0170	83.51
6	19.20	9.60	0.1676	0.9860	0.9734	0.0170	83.66
12	19.20	9.60	0.1676	0.9860	0.9712	0.0170	83.85
24	19.20	9.60	0.1676	0.9860	0.961	0.0168	84.74

Table S8. Crystallite size (020)

Cycles	2Θ, °	Θ, °	Θ, radians	cos Θ	FWHM, °	FWHM, radians	Size, nm
0	9.24	4.62	0.0806	0.9968	1.1047	0.0193	72.92
3	9.24	4.62	0.0806	0.9968	1.1666	0.0204	69.05
6	9.24	4.62	0.0806	0.9968	1.3696	0.0239	58.82
12	9.24	4.62	0.0806	0.9968	1.2166	0.0212	66.21
24	9.24	4.62	0.0806	0.9968	1.2802	0.0223	62.92

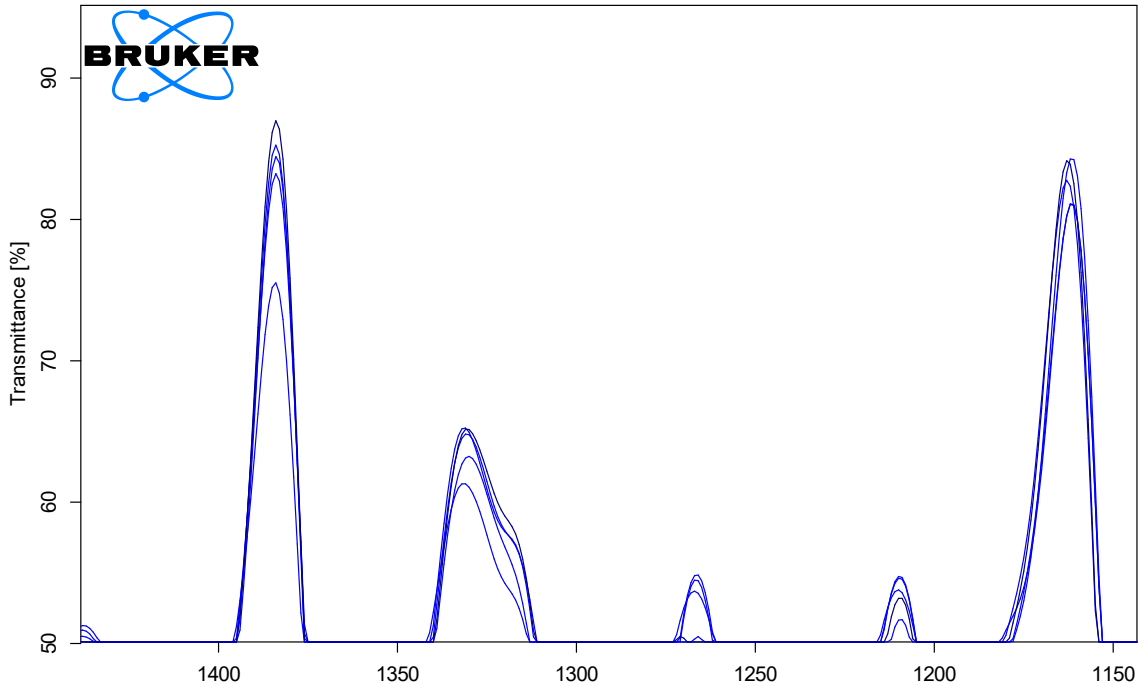

Figure S12. The first derivative of the digitally filtered FT-IRs (a 17-point Savitzky-Golay digital filter applied) for C0, 5 spectra.

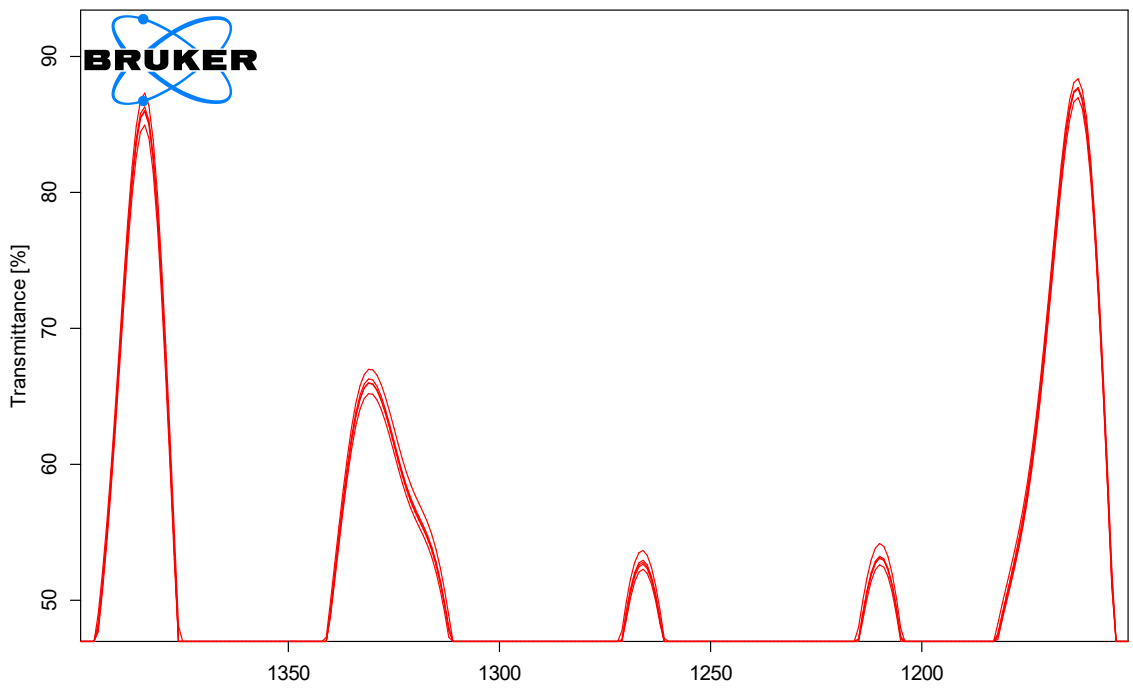

Figure S13. The first derivative of the digitally filtered FT-IRs (a 17-point Savitzky-Golay digital filter applied) for C3, 5 spectra.

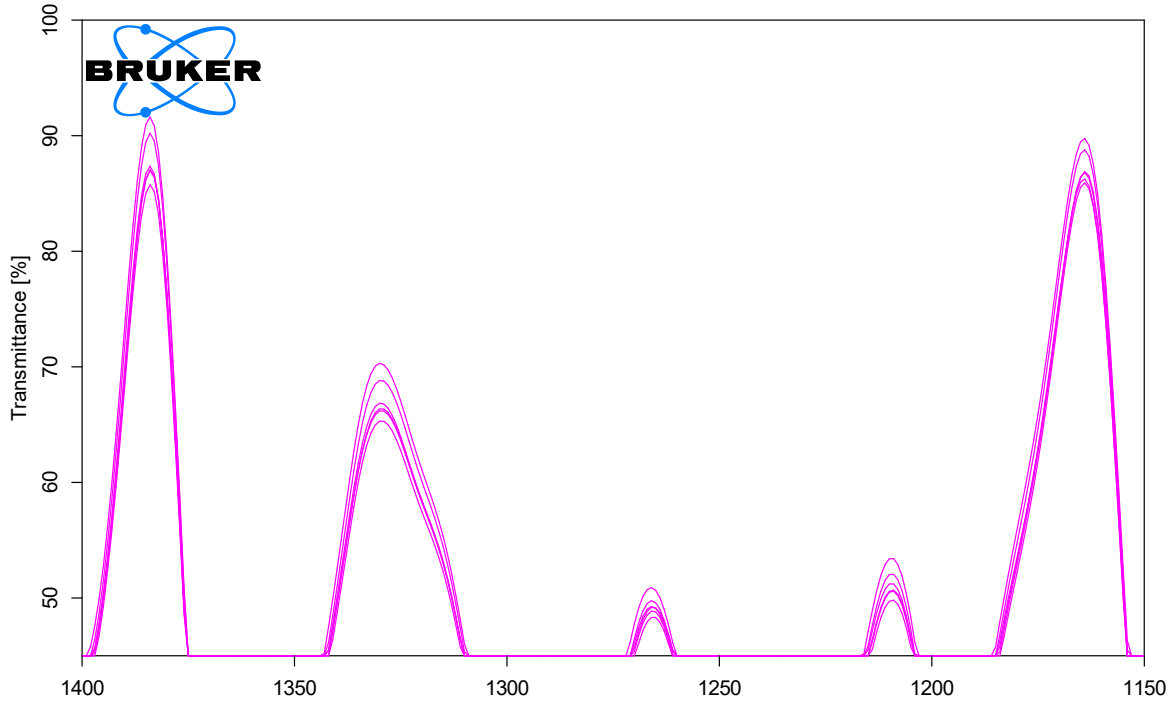

Figure S14. The first derivative of the digitally filtered FT-IRs (a 17-point Savitzky-Golay digital filter applied) for C6, 5 spectra.

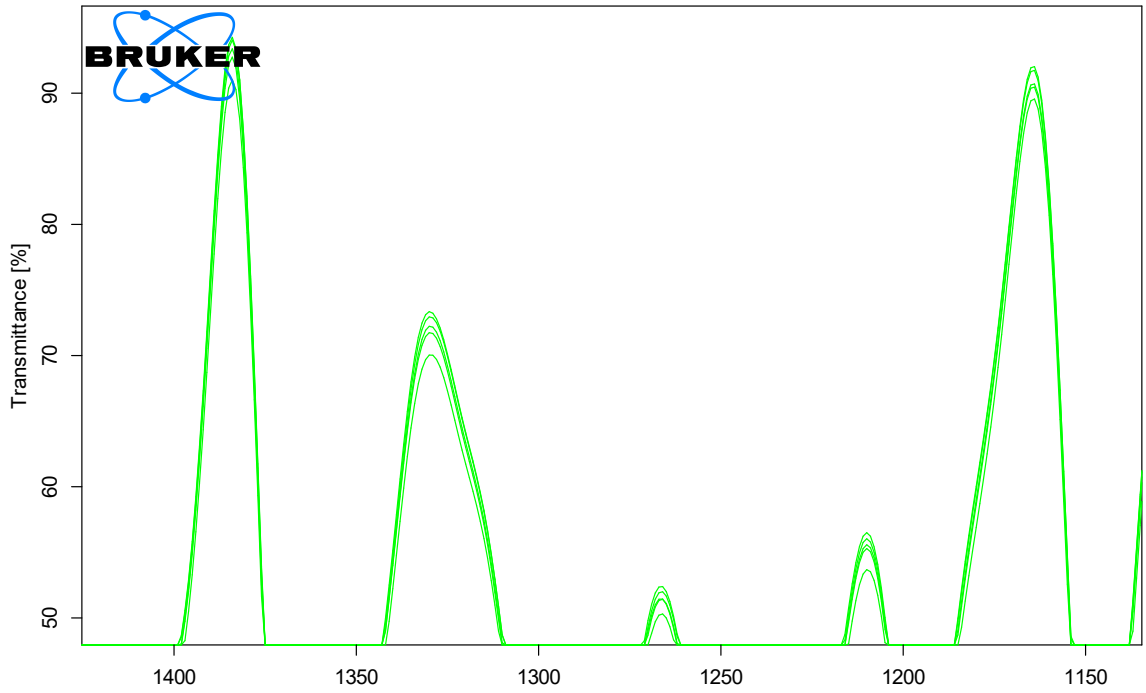

Figure S15. The first derivative of the digitally filtered FT-IRs (a 17-point Savitzky-Golay digital filter applied) for C12, 5 spectra.

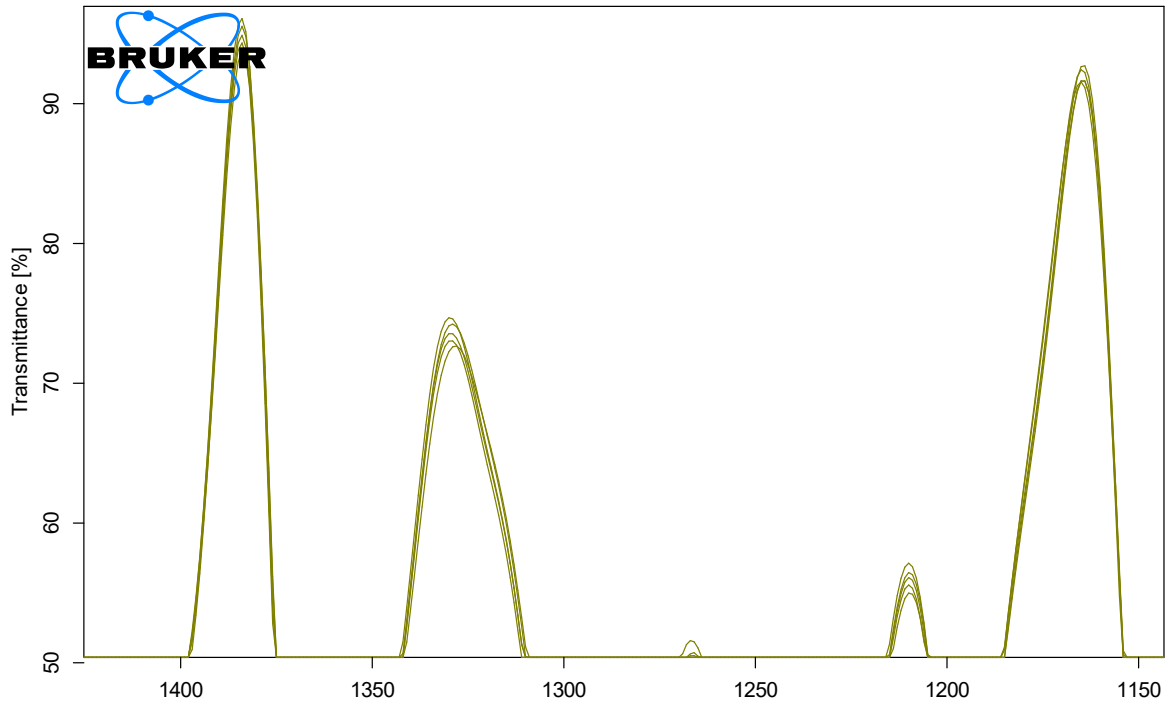

Figure S16. The first derivative of the digitally filtered FT-IRs (a 17-point Savitzky-Golay digital filter applied) for C24, 5 spectra.

Table S9. The intensity of the peaks MB_1 (1383 cm^{-1}), MB_2 (1327 cm^{-1}), and RB (1163 cm^{-1}) and %DA for C0 – C24.

Sample	Trial	MB_1 at 1383 cm^{-1}	MB_2 at 1327 cm^{-1}	RB at 1163 cm^{-1}	DA, %[a]	STD.
C0	Rep. 1	87.14	65.08	84.11	84.25	87.14
	Rep. 2	85.20	65.08	84.23	82.62	85.20
	Rep. 3	84.23	64.78	82.78	83.64	84.23
	Rep. 4	83.20	63.26	81.20	83.87	83.20
	Rep. 5	75.57	61.20	81.20	76.26	75.57
	Average				**82.13**	**2.98**
C3	Rep. 1	87.22	66.91	88.09	80.42	
	Rep. 2	86.28	66.10	87.47	79.94	
	Rep. 3	85.78	65.85	87.47	79.40	
	Rep. 4	85.78	65.85	87.47	79.39	
	Rep. 5	84.84	65.16	86.78	79.08	
	Average				**79.65**	**0.48**
C6	Rep. 1	91.93	70.24	89.64	84.22	
	Rep. 2	90.08	68.69	88.30	83.50	
	Rep. 3	87.27	66.69	86.60	82.21	
	Rep. 4	87.28	66.32	86.08	82.86	
	Rep. 5	85.64	65.28	85.57	81.33	
	Average				**82.82**	**1.00**
C12	Rep. 1	94.08	73.31	91.05	86.08	
	Rep. 2	93.30	72.78	91.53	84.56	
	Rep. 3	92.64	72.26	90.48	85.06	
	Rep. 4	92.64	71.80	90.41	84.83	
	Rep. 5	91.26	70.03	89.30	84.03	
	Average				**84.91**	**0.68**
C24	Rep. 1	95.83	74.64	95.73	82.41	
	Rep. 2	93.30	74.14	92.13	84.74	
	Rep. 3	95.20	73.52	91.44	86.50	
	Rep. 4	94.70	73.14	91.37	85.98	
	Rep. 5	93.57	72.58	91.37	84.80	
	Average				**84.89**	**1.41**

[a] Calculated using the equation: $\%DA = \frac{\frac{(MB1 + MB2)}{RB} - 0.487\%}{0.0157}$

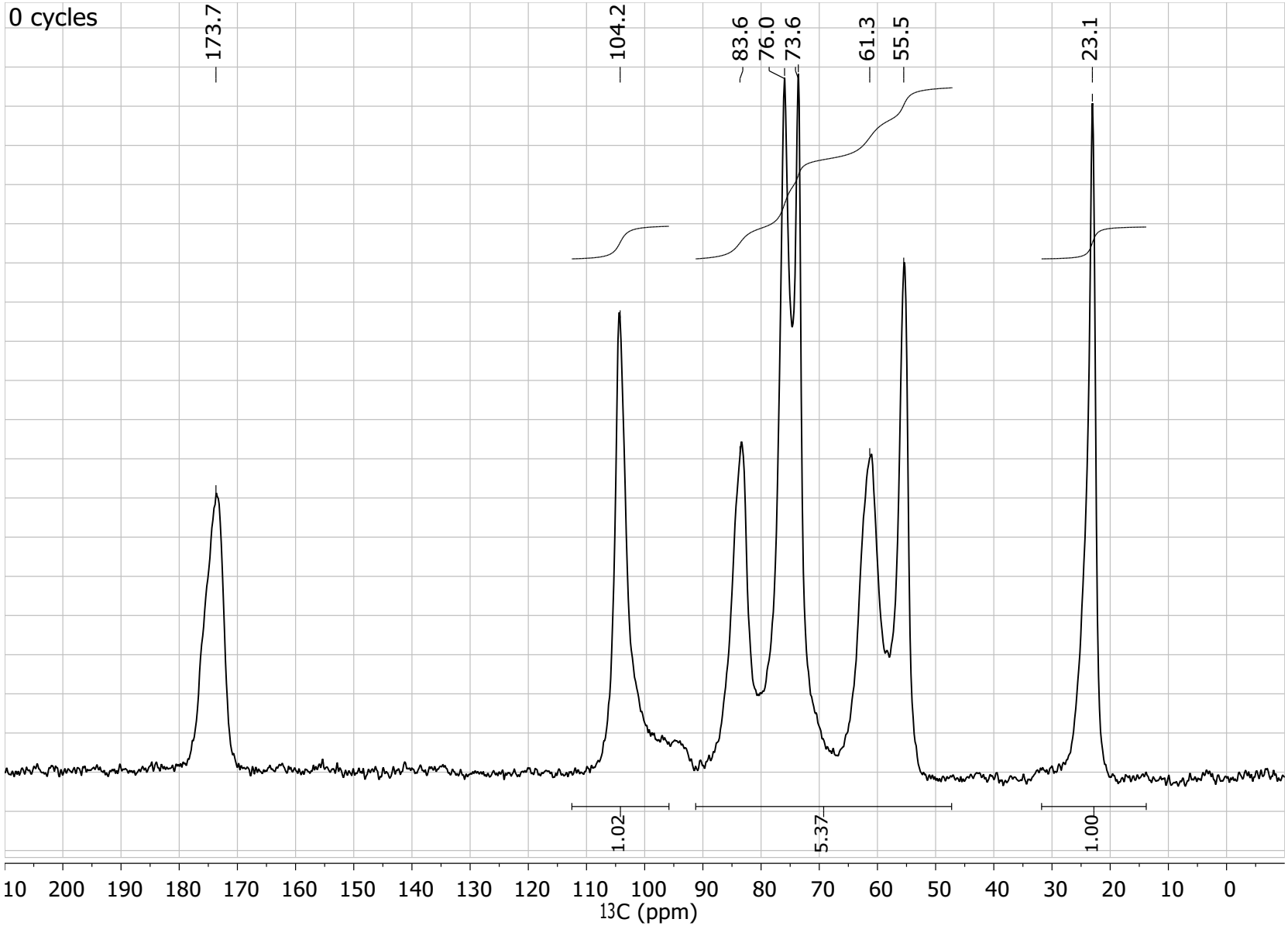

Figure S15. Solid-state Cross-Polarization Magic Angle Spinning Carbon-13 Nuclear Magnetic Resonance (CP MAS NMR) spectrum for C0.

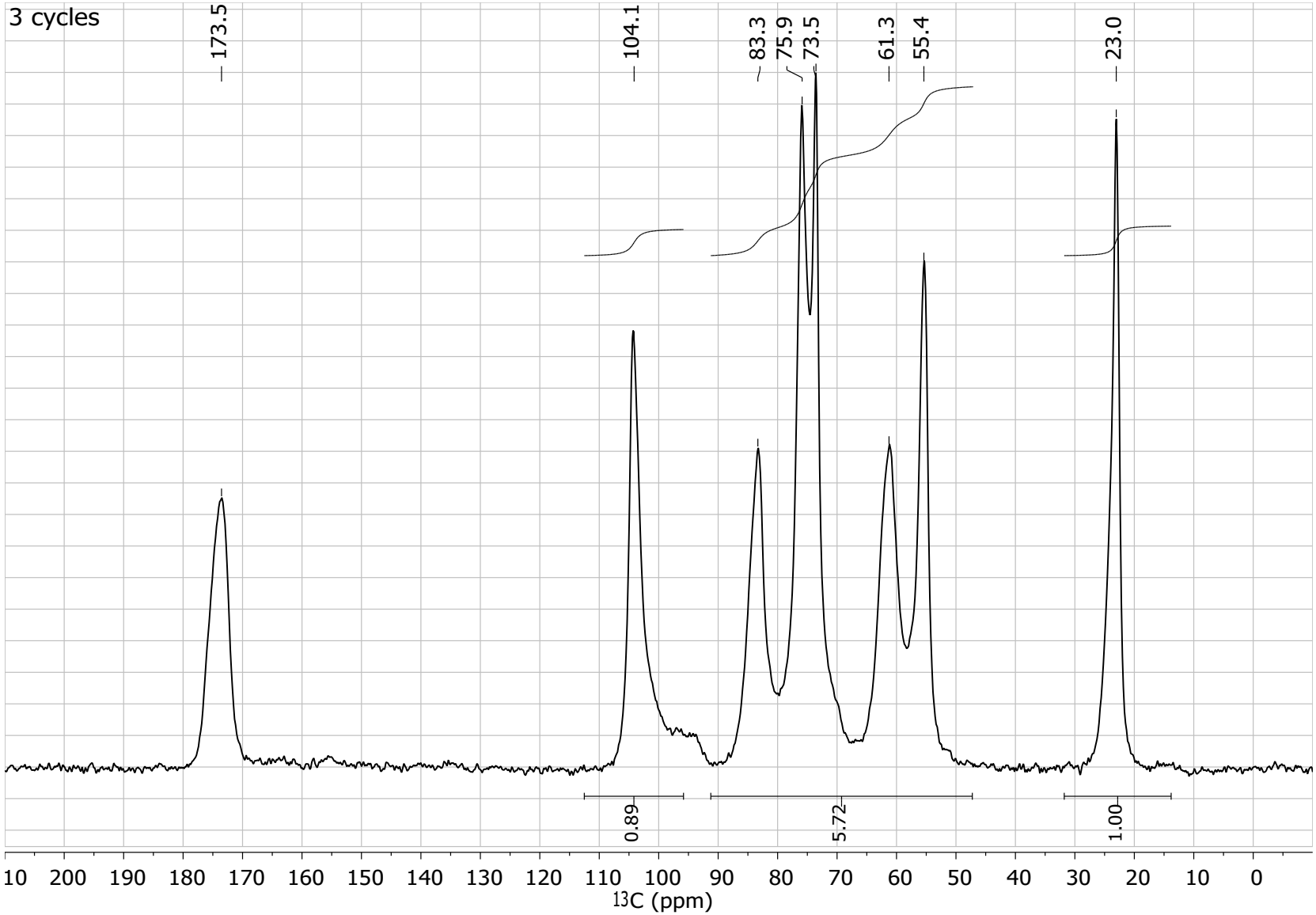

Figure S16. Solid-state Cross-Polarization Magic Angle Spinning Carbon-13 Nuclear Magnetic Resonance (CP MAS NMR) spectrum for C3.

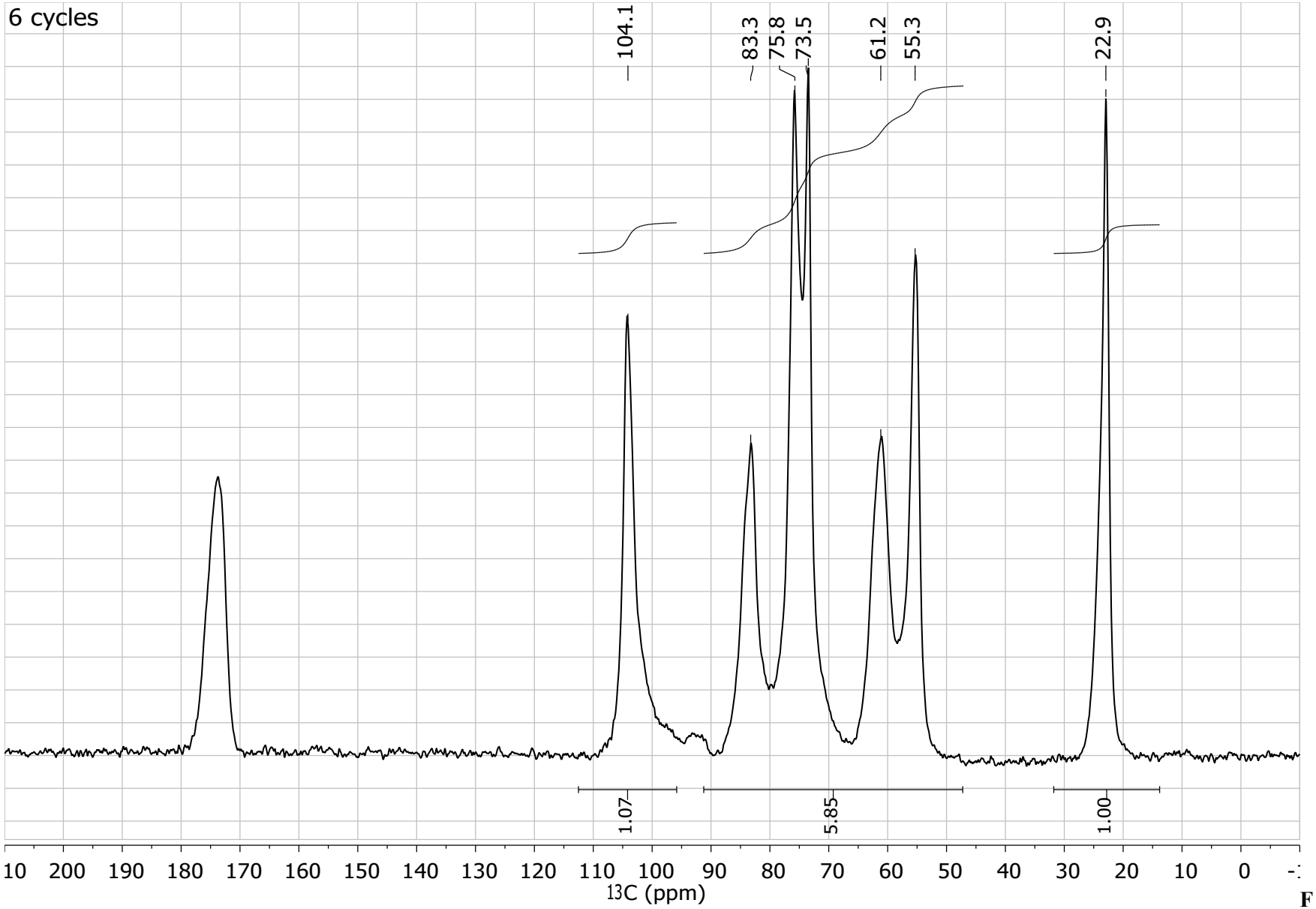

F igure S17. Solid-state Cross-Polarization Magic Angle Spinning Carbon-13 Nuclear Magnetic Resonance (CP MAS NMR) spectrum for C6.

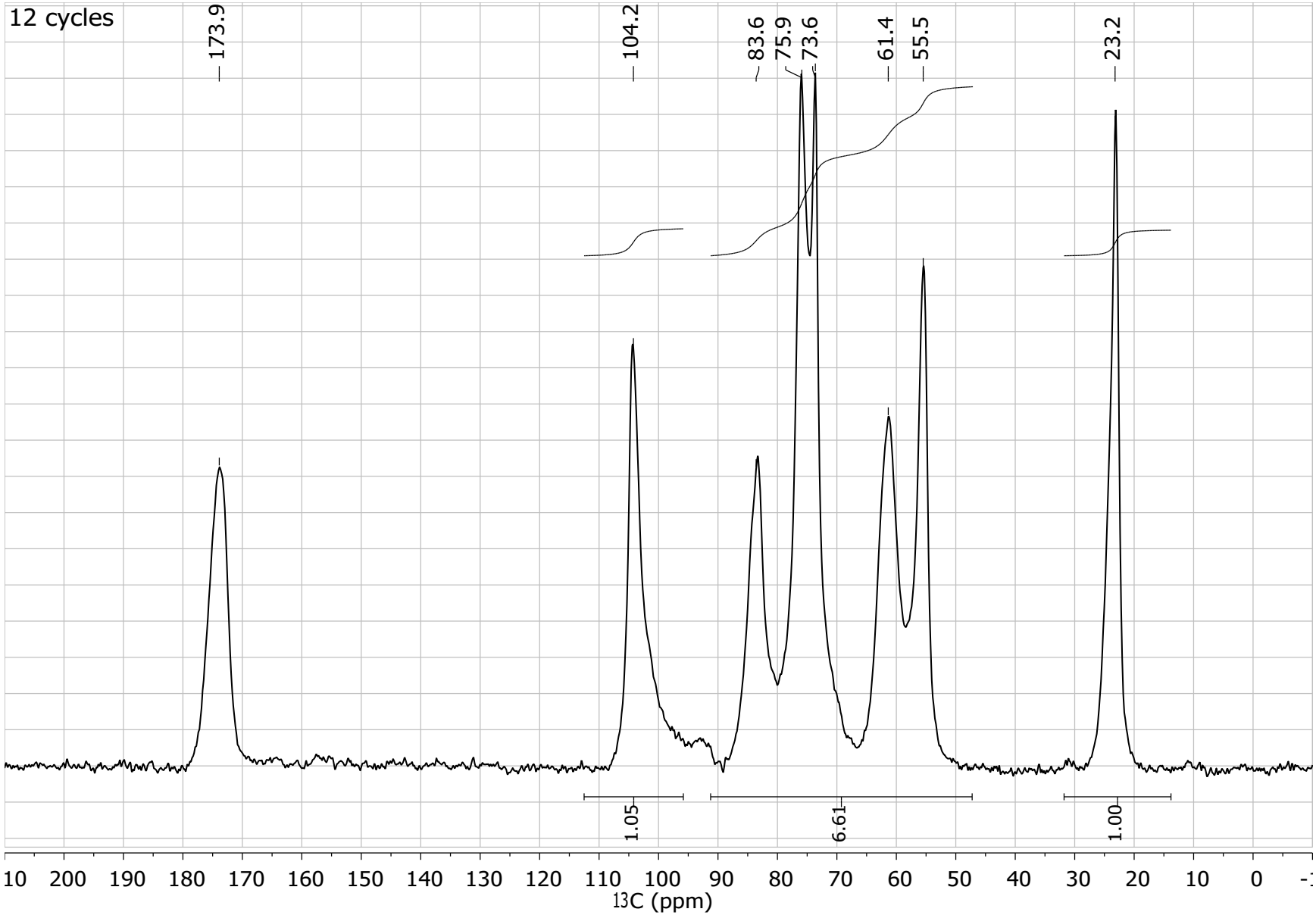

Figure S18. Solid-state Cross-Polarization Magic Angle Spinning Carbon-13 Nuclear Magnetic Resonance (CP MAS NMR) spectrum for C12.

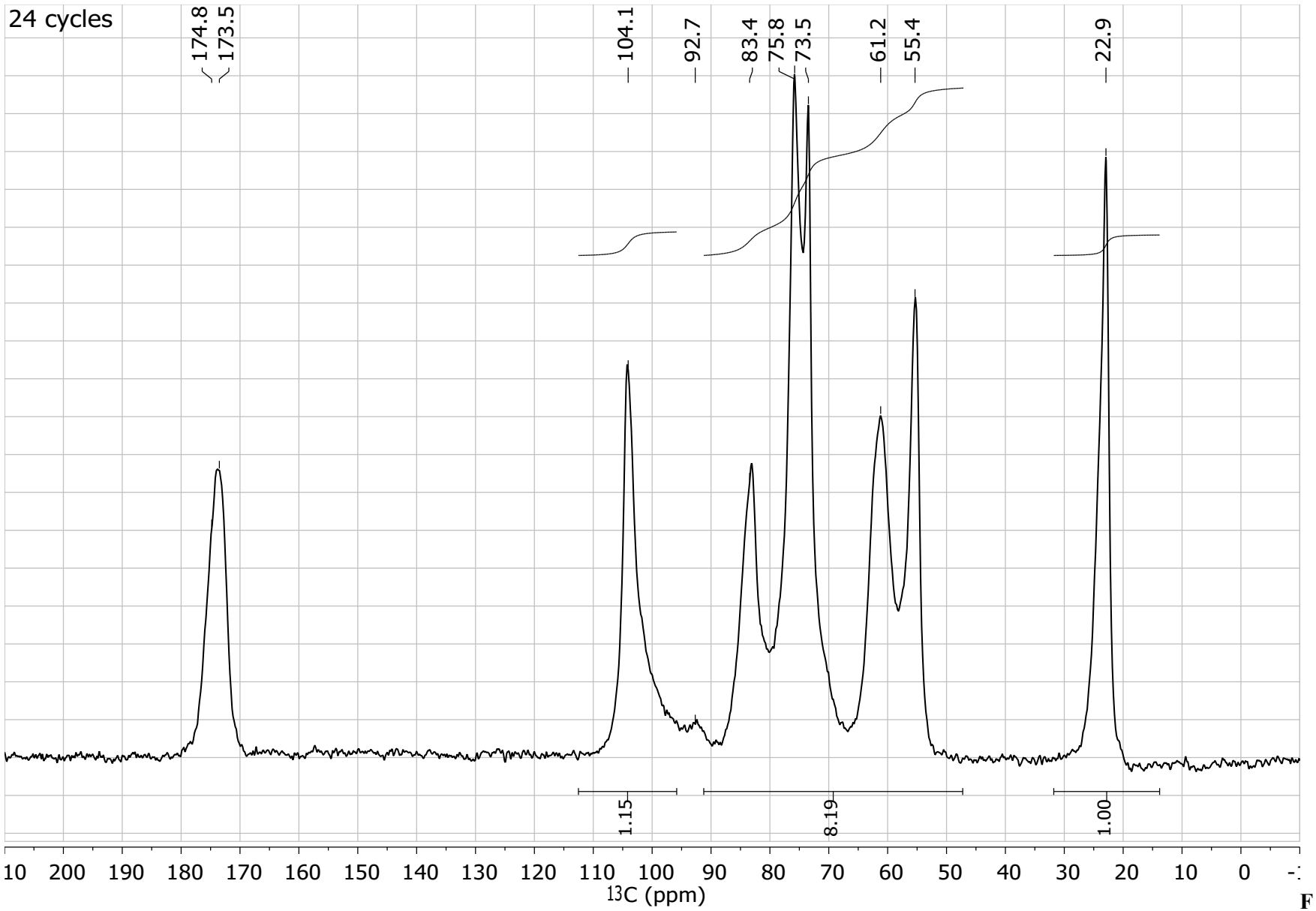

F igure S19. Solid-state Cross-Polarization Magic Angle Spinning Carbon-13 Nuclear Magnetic Resonance (CP MAS NMR) spectrum for C24.

Table S10. %DA calculated from Solid-state Cross-Polarization Magic Angle Spinning Carbon-13 Nuclear Magnetic Resonance (CP MAS NMR) spectrum for C24

Sample	With Baseline Correction	
	Integral Ratio	%DA
C0	5.37	0.93
C3	5.72	0.87
C6	5.85	0.85
C12	6.61	0.76
C24	8.19	0.61

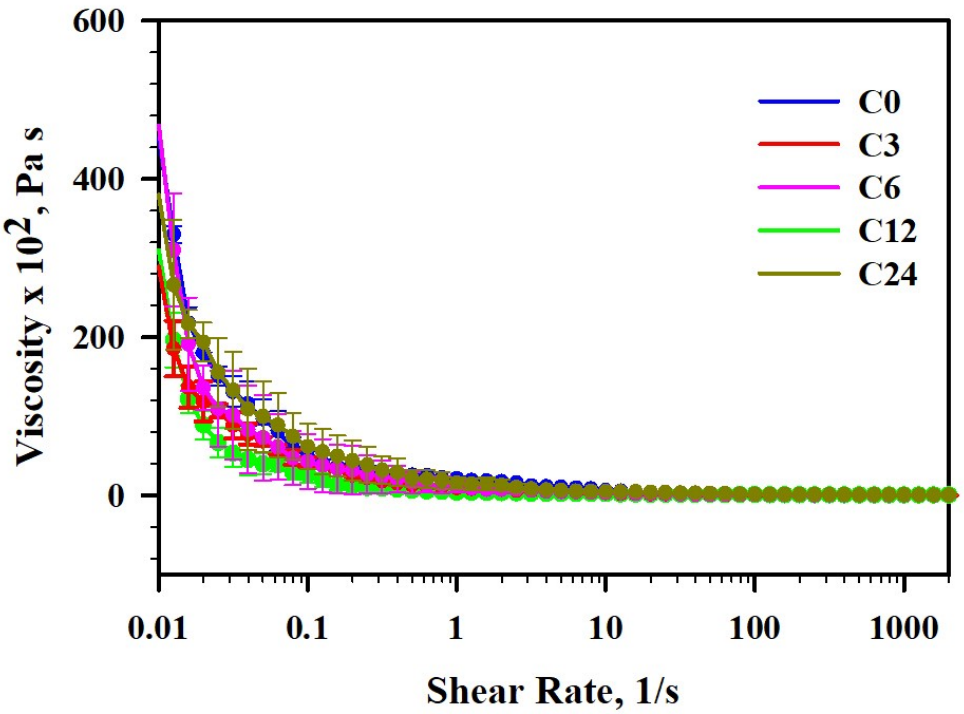

Figure S20. Flow curves for 1 wt% chitin solutions in ionic liquid 1-ethyl-3-methylimidazolium acetate [C_2mim][OAc]: C0 (blue), C3 (red), C6 (pink), C12 (green), and C24 (mustard), baseline corrected and normalized.

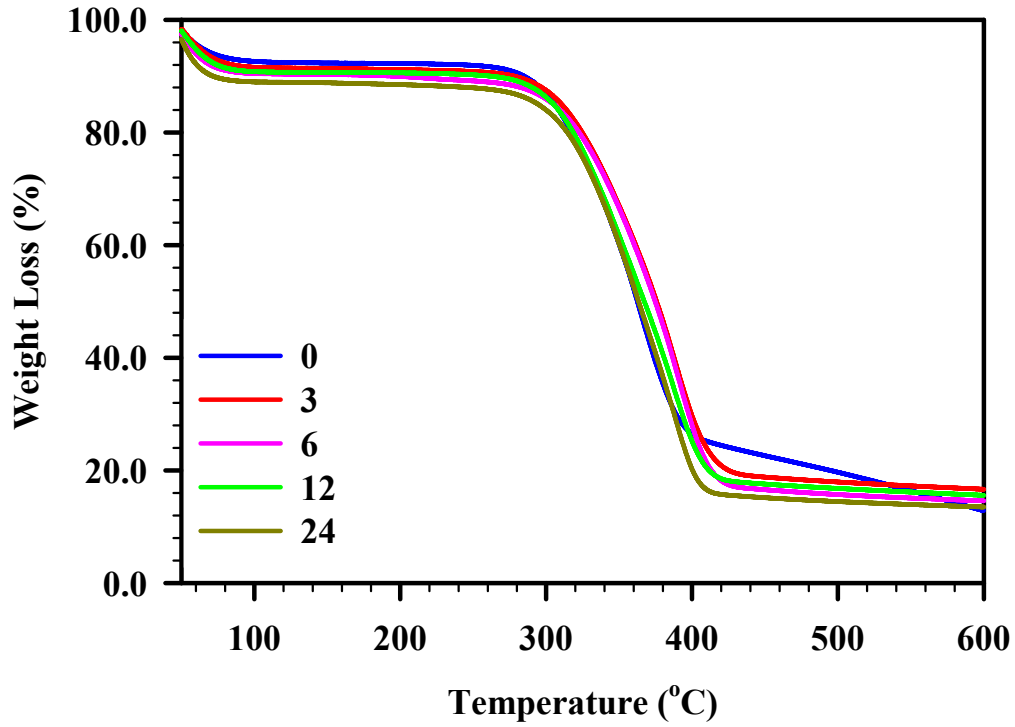

Figure S21. TGA curves for cryoground chitin: C0 (blue), C3 (red), C6 (pink), C12 (green), and C24 (mustard), baseline corrected and normalized.

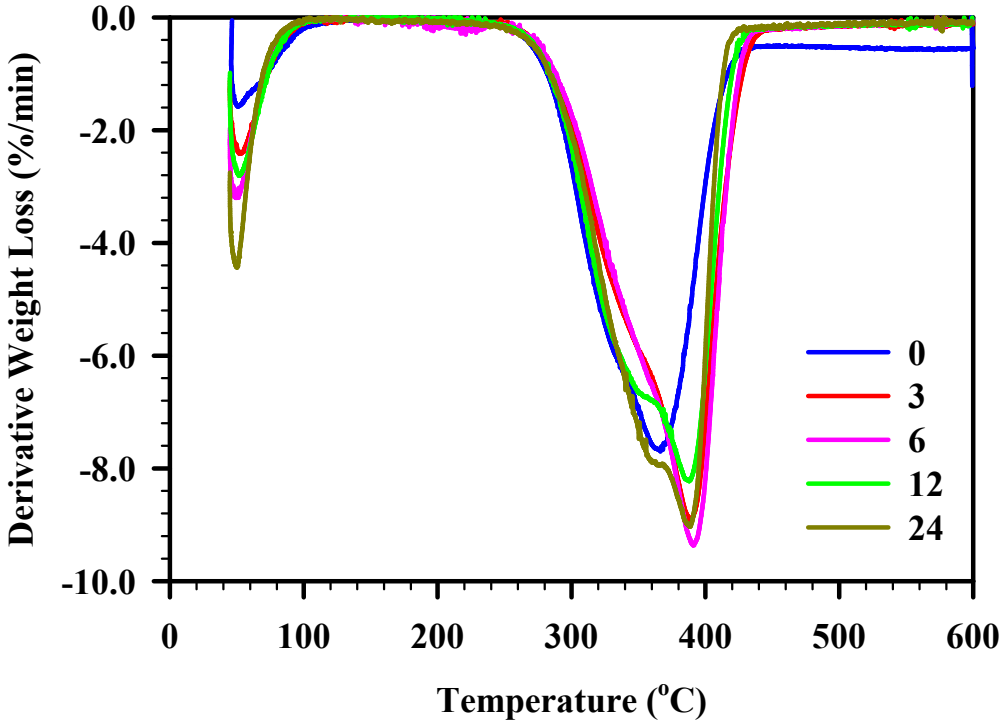

Figure S22. DTG curves for cryoground chitin: C0 (blue), C3 (red), C6 (pink), C12 (green), and C24 (mustard), baseline corrected and normalized.

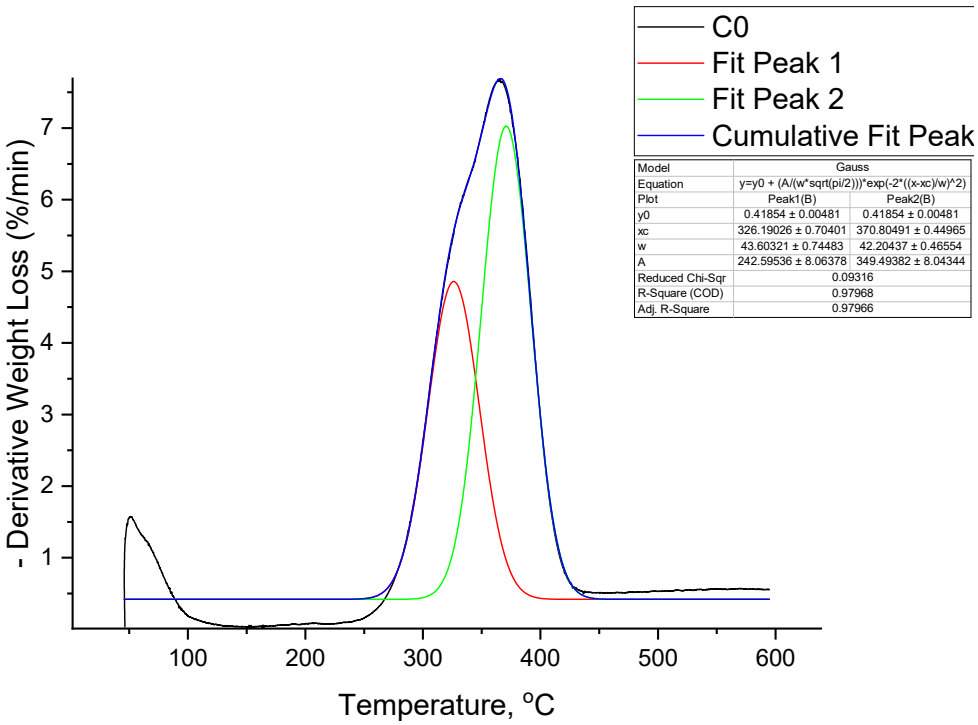

Figure S23. DTG curve and peak fitting for cryoground chitin: C0.

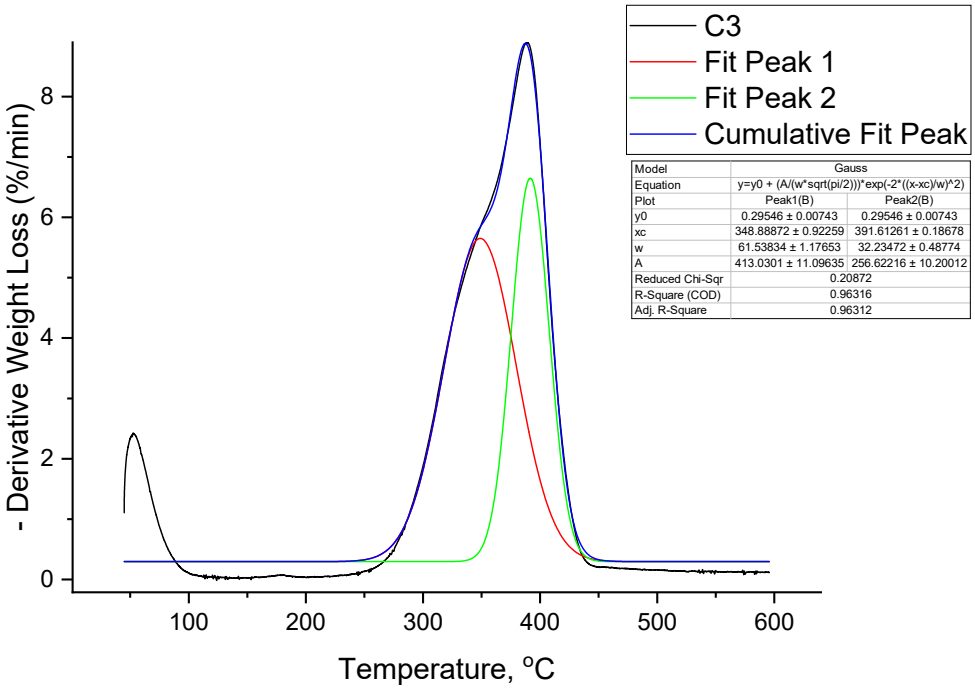

Figure S24. DTG curve and peak fitting for cryoground chitin: C3.

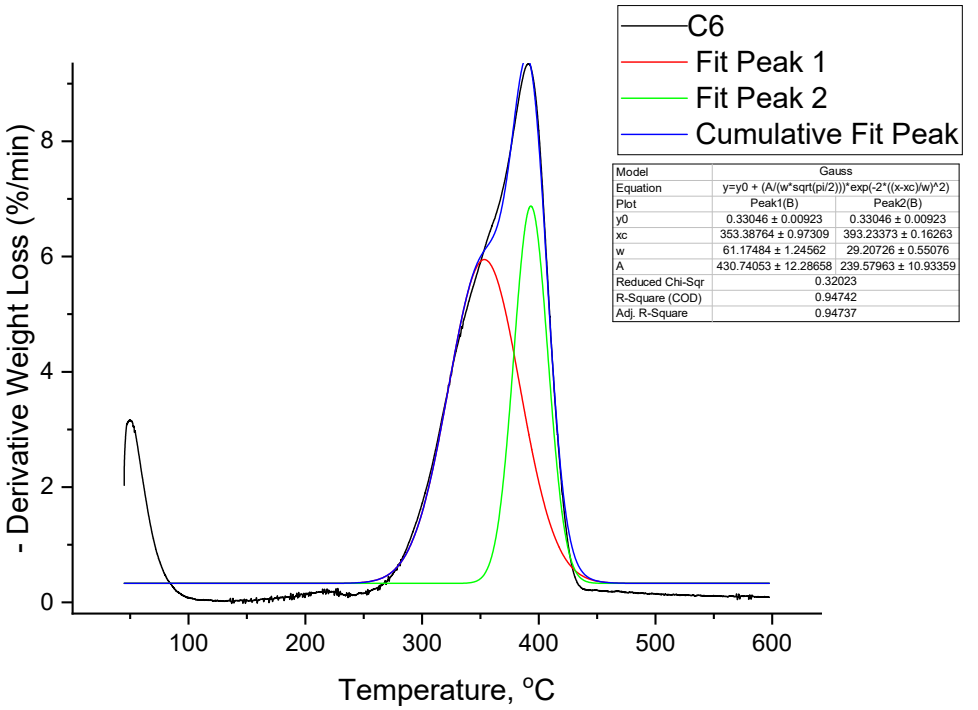

Figure S25. DTG curve and peak fitting for cryoground chitin: C6.

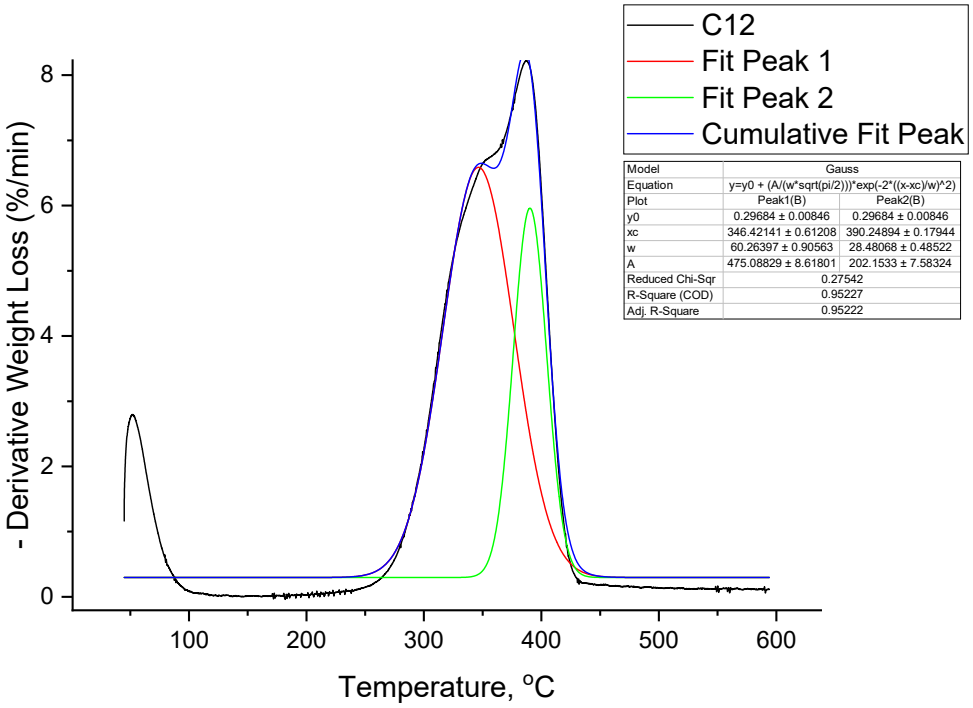

Figure S26. DTG curve and peak fitting for cryoground chitin: C12.

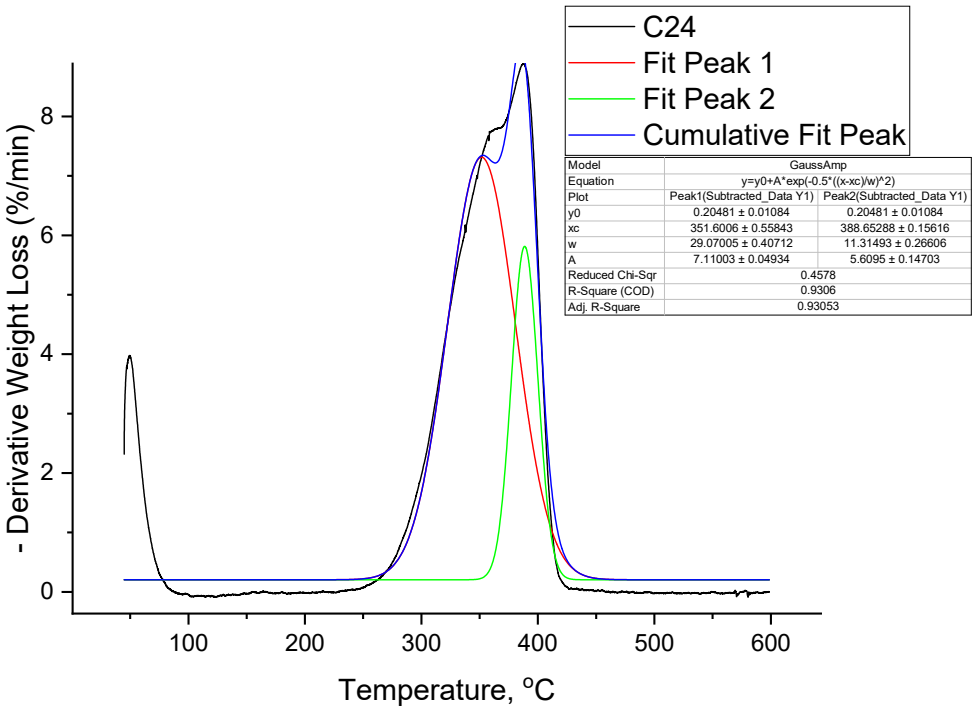

Figure S27. DTG curve and peak fitting for cryoground chitin: C24.

REFERENCES

[i] G. Cárdenas, G. Cabrera, E. Taboada, S. P. Miranda, *J. Applied Polym. Sci*., 2004, 1876 – 1885.

[ii] M. Kaya, M. Mujtaba, H. Ehrlich, A. M. Salaberria, T. Baran, C. T. Amemiya, R. Galli, L. Akyuzh, I. Sargin, J. Labidi, *Carbohydr. Polym*., 2017, **176**, 177 – 186.

[iii] I. Akpan, O. P. Gbenebor, S. O. Adeosun, *Int. J. Biol. Macromol*., 2018, **106**, 1080 – 1088.